



ELSEVIER

Available online at [www.sciencedirect.com](http://www.sciencedirect.com)

SCIENCE @ DIRECT®

Proceedings of the Combustion Institute 30 (2005) 1371–1379

Proceedings  
of the  
Combustion  
Institute

[www.elsevier.com/locate/proci](http://www.elsevier.com/locate/proci)

# The effects of pressure on the yields of polycyclic aromatic hydrocarbons produced during the supercritical pyrolysis of toluene

Elmer B. Ledesma<sup>a</sup>, Mary J. Wornat<sup>a,\*</sup>, Philip G. Felton<sup>b</sup>,  
Joseph A. Sivo<sup>b</sup>

<sup>a</sup> Department of Chemical Engineering, Louisiana State University, Baton Rouge, LA 70803, USA

<sup>b</sup> Department of Mechanical and Aerospace Engineering, Princeton University, Princeton, NJ 08544, USA

## Abstract

To understand better the reactions leading to polycyclic aromatic hydrocarbons (PAH)—and ultimately carbonaceous solids—within the context of supercritical fuel pyrolysis, we have pyrolyzed the model fuel toluene (critical temperature, 319 °C; critical pressure, 41 atm) in an isothermal silica-lined stainless steel coil reactor at 535 °C, 140 s, and pressures of 20–100 atm. Analysis of the reaction products by gas chromatography and high-pressure liquid chromatography reveals that the yields of benzene and 27 individual PAH increase exponentially with pressure. For 26 of these 28 products, the experimentally measured yield/pressure data conform well to a first-order global kinetics model—permitting determination of the preexponential factor  $A$  and the activation volume  $\Delta V^\ddagger$ , which appear in the pressure-dependent expression for the kinetic rate constant:  $k = A \exp[(-\Delta V^\ddagger/RT)p]$ . For most of the PAH, derived values of  $\Delta V^\ddagger$  lie between  $-2.5$  and  $-4$  L/mol, signifying the doubling of PAH formation rates by pressure increases of only 18.4 or 11.5 atm, respectively. Some of the larger PAH, such as the 8-ring benzo[*a*]coronene and the 9-ring naphtho[8,1,2-*abc*]coronene, exhibit negative activation volumes of even greater magnitude—a result of particular relevance to the formation of carbonaceous solids, as large PAH are thought to be precursors to these solids. The PAH yield data also reveal product yield ratios, within certain PAH isomer families, that are peculiar to the high-pressure supercritical pyrolysis environment—suggesting that mechanisms for PAH formation differ significantly from those in atmospheric-pressure gas-phase pyrolysis environments. © 2004 The Combustion Institute. Published by Elsevier Inc. All rights reserved.

**Keywords:** Polycyclic aromatic hydrocarbons; Supercritical fuel pyrolysis; Toluene; Pressure effects; Global kinetic rate parameters

## 1. Introduction

The fuels used in the next generation of hypersonic aircraft will have to operate under very high

pressures and will have to sustain very high heat loads in order to meet aircraft cooling requirements [1,2]. Within the fuel lines and injection system, where residence times can be several minutes, fuel temperatures and pressures may reach or exceed 540 °C and 150 atm [1]—temperatures and pressures that exceed the critical temperatures and pressures of most pure hydrocarbons and jet

\* Corresponding author. Fax: +1 225 578 1476.  
E-mail address: [mjwornat@lsu.edu](mailto:mjwornat@lsu.edu) (M.J. Wornat).

fuels [2,3]. At these temperatures and pressures, the fuel can undergo pyrolytic reactions, which have the potential of forming carbonaceous solid deposits that can clog fuel lines, foul fuel nozzles, and lead to undesirable or even disastrous effects for the aircraft. To develop reliable fuel systems that will not be subject to solid deposit formation, we need a thorough understanding of the pyrolysis behavior of candidate fuels under the supercritical conditions that they will be operating. Of particular interest are the reactions leading to polycyclic aromatic hydrocarbons (PAH), which can serve as precursors to the carbonaceous solids [4].

The fact that the fuel pyrolysis environment is a supercritical one introduces several complexities. Solvent–solute interactions, absent in the gas phase, can exhibit huge effects in supercritical fluids, often affecting chemical reaction pathways by facilitating the formation of certain transition states [5–11]. Because solvent–solute interactions are very dependent on pressure, chemical reaction rates in supercritical fluids are highly pressure-dependent [5–13]; the kinetic rate constant has been shown [10,12] to vary exponentially with pressure.

For the case of fuel pyrolysis reactions, Stewart et al. [4,14] have demonstrated that reaction pathways and reaction kinetics indeed differ between the gas phase and the supercritical phase. Their pyrolysis experiments with decalin and methylcyclohexane in an atmospheric-pressure flow reactor and in the supercritical pyrolysis reactor currently in our use show that under supercritical conditions—but not in the gas phase at atmospheric pressure—both decalin and methylcyclohexane are able to produce methylated C<sub>5</sub>-ring intermediates that readily convert to structures containing 6-membered aromatic rings. These aromatic rings then serve as kernels for further cyclic growth to PAH and ultimately carbonaceous solids. For the same two fuels, Stewart et al. [4,14] also report different global Arrhenius kinetic rate parameters  $A$  and  $E_a$  for supercritical pyrolysis experiments, compared to gas-phase experiments—substantiating the fact that reaction kinetics, as well as reaction pathways, differ significantly for the two phases. Therefore, even for fuels whose gas-phase pyrolysis behavior is well understood, it is of critical importance to study their pyrolysis in the supercritical phase, if these fuels are to be considered for supercritical applications.

To that end, we have conducted supercritical pyrolysis experiments with the model fuel toluene (critical temperature, 319 °C; critical pressure, 41 atm), an aromatic component of jet fuels [15]. Use of a model fuel facilitates our ability to trace reaction pathways from starting material to PAH to carbonaceous solids—increasing the opportunity to gain understanding of the fundamental reaction processes taking place. Future plans to combine toluene with other components will con-

tribute to a better understanding of fuels that are more complex mixtures. Gas-phase toluene pyrolysis has been investigated by several researchers [16–19], but little is known about the pyrolysis of toluene under supercritical conditions. Likewise, most research on PAH formation pertains to the gas phase [20–35]; little has been done under supercritical conditions.

Our supercritical toluene pyrolysis experiments make use of the reactor designed by Davis [36] and used by Stewart et al. [4,14] for supercritical pyrolysis experiments with other model fuels. Since the main focus of our work is the formation of PAH as precursors to carbonaceous solids, a critical component of our work is the chemical analysis of large PAH, for which we employ high-pressure liquid chromatography (HPLC) with diode-array ultraviolet–visible (UV) absorption detection, a technique ideally suited for isomer-specific PAH analysis.

The results of our supercritical toluene pyrolysis experiments to date are presented in three papers. The first [37] provides the chromatographic and spectroscopic evidence documenting the unequivocal identification of the PAH products. The second [38] reports the yields of one-ring aromatics and bi-toluyls, proposing reaction schemes for these species' participation in PAH formation. In this the third paper, we report the yields, versus pressure, of benzene and 27 PAH produced from the pyrolysis of toluene at 535 °C, 140 s, and pressures of 20–100 atm. For 26 of these aromatic products, we also report kinetic rate parameters for the pressure-dependent first-order global kinetic rate expressions for the formation of these products.

## 2. Experimental equipment and techniques

The supercritical toluene pyrolysis experiments are conducted in an isothermal, isobaric reactor designed expressly for such experiments by Davis [36] and used by Stewart [4,14] for supercritical pyrolysis of decalin, tetralin, and methylcyclohexane. The reactor system is illustrated in Fig. 1. Prior to an experiment, liquid toluene (99.9+% pure) is sparged with nitrogen for three hours, as described by Stewart [4], to get rid of any dissolved oxygen that could introduce auto-oxidative effects [3]. The sparged fuel is then loaded into a high-pressure nonreciprocating pump that delivers the fuel to the reactor, as shown in Fig. 1. The reactor itself is a coil of 1-mm i.d., 1.59-mm o.d. capillary tube made of silica-lined stainless steel. (The silica lining prevents wall-catalyzed deposit formation that occurs with unlined stainless steel [3,4,36].) The reactor coil is immersed in a temperature-controlled fluidized-alumina bath, which ensures isothermality throughout the reactor length. As indicated in Fig. 1, the entrance

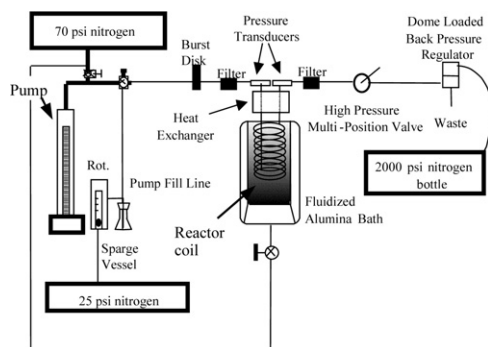


Fig. 1. Reactor system for supercritical pyrolysis experiments. Adapted from Stewart [4].

and exit lines of the reactor are passed through a water-cooled (20 °C) heat exchanger to ensure a controlled thermal history and residence time. Exiting the heat exchanger, the quenched reaction products pass through a stainless steel filter (hole size, 5  $\mu\text{m}$ ) and on to a six-position high-pressure valve for product collection. A dome-loaded back-pressure regulator, downstream of the valve, controls the system pressure, to within  $\pm 0.2$  atm, up to a maximum of 110 atm. A burst disk, located upstream of the reactor, provides a safe flow outlet, in case of over-pressurization.

As documented by Stewart [4] and Davis [36], the reactor has been designed to meet Cutler's [39] and Lee's [40] criteria for idealization as plug flow, with regard to species concentration profiles—criteria concerning the product of the Reynolds and Schmidt numbers [40], criteria for fast radial species diffusion relative to forced convection, and criteria for minimum axial diffusion relative to axial convection [39]. The resulting radially uniform species concentrations, coupled with the reactor's constant-temperature and constant-pressure operation, render this reactor ideal for supercritical pyrolysis kinetics experiments. The reactor system is capable of operating at temperatures up to 590 °C, pressures up to 110 atm, and residence times up to 3600 s—operating ranges relevant to those envisioned for fuel systems in future hypersonic aircraft [1]. The toluene pyrolysis experiments reported here are conducted at a fixed temperature of 535 °C and a fixed residence time of 140 s, corresponding to a reactor coil length of 2.44 m. Each experiment is run isobarically; pressure is varied, from experiment to experiment, over the range of 20–100 atm.

At the conclusion of each pyrolysis experiment, the reaction products are removed from the high-pressure collection valve and transferred to a vial. To analyze the smaller aromatic products, two separate 10- $\mu\text{L}$  aliquots of the product solution are removed for injection onto a gas chromatograph. The remainder of the product

solution ( $\sim 1$  mL) is prepared for HPLC, which analyzes the larger aromatic products.

Gas chromatographic analysis of the supercritical fuel pyrolysis products is performed on an Agilent Model 6890 gas chromatograph (GC) with a flame-ionization detector (FID), in conjunction with an Agilent Model 5973 mass spectrometer (MS). A sample volume of 10  $\mu\text{L}$  is injected by syringe, through a split injector, onto a HP-5 fused silica capillary column of length, 30 m; diameter, 0.25 mm; and film thickness, 0.1  $\mu\text{m}$ . The column temperature is programmed to hold at 40 °C for the first 3 minutes; it is then ramped at 4 °C/min to 300 °C, where it is held for 15 minutes. The GC/FID/MS instrument is used to quantify 1- to 3-ring aromatic products, plus two 4-ring species, pyrene and fluoranthene. The products are identified by matching retention times and mass spectra with those of reference standards, and quantification is achieved by calibrating the GC with injections of reference standards of known concentrations.

The portion of the product solution reserved for HPLC analysis is concentrated in a Kuderna–Danish apparatus and exchanged, under nitrogen, into 100  $\mu\text{L}$  dimethyl sulfoxide, a solvent compatible with the solvents used in the HPLC method employed for PAH analysis. During the concentration and solvent-exchange procedure, portions of the more volatile aromatics, such as the 1- and 2-ring species, are lost to vaporization; hence, these lighter aromatic products are quantified by gas chromatographic analysis, as described above.

For analysis of the large aromatic products (all products of  $\geq 4$  rings, except pyrene and fluoranthene) by HPLC, a 20- $\mu\text{L}$  aliquot of the product/dimethyl sulfoxide solution is injected onto a Hewlett–Packard Model 1050 high-pressure liquid chromatograph, coupled to a diode-array UV absorbance detector. The chromatographic separation method [22,41] utilizes a reversed-phase Vydac 201-TP octadecylsilica column of particle size, 5  $\mu\text{m}$ ; inner diameter, 4.6 mm; and length, 250 mm. A time-programmed sequence of solvents—acetonitrile/water, acetonitrile, and dichloromethane—is pumped through the column, and the PAH product components elute in the order of increasing molecular size. UV absorbance spectra are taken, every 0.6 s, of the exiting components, which are then identified by matching HPLC elution times and UV absorbance spectra (unique to each PAH) with those of PAH reference standards. As documented in our product identification paper [37], our reference standards include both commercially available compounds as well as PAH that have been specially synthesized for our identification efforts. Quantification of the identified PAH comes from extensive calibration of the HPLC/UV instrument with the reference standards, taking into account nonlin-

earities in the response of diode-array detectors at high analyte concentrations [42].

### 3. Results and discussion

The highest-yield aromatic products from our supercritical toluene pyrolysis experiments are benzene, the three xylenes, ethyl benzene, and the ten bi-toluyis—whose yields are reported and discussed in another paper [38]. Figs. 2–8 present the yields, versus pressure, of benzene and the 27 PAH unequivocally identified [37] in the products of supercritical toluene pyrolysis at 535 °C and 140 s. The PAH range in size from 2 to 10 fused aromatic rings and are grouped as follows: Fig. 2—benzene, naphthalene, indene, and fluorene; Fig. 3—phenanthrene, anthracene, chrysene, and benz[*a*]anthracene; and Fig. 4—pyrene and three pyrene benzologues; Fig. 5—fluoranthene and three fluoranthene benzologues; Fig. 6—benzo[*ghi*]perylene and three of its benzologues; Fig. 7—methyl-naphthalenes and -anthracenes; and Fig. 8—1-methylpyrene, 1-methylcoronene, and two large unsubstituted PAH. In each of the plots of Figs. 2–8, the filled circles are experimentally measured points. Except for Fig. 8C and D, all of the curves in Figs. 2–8 represent fits of the data to first-order global kinetics expressions, as explained below. In Fig. 8C and D, the lines are

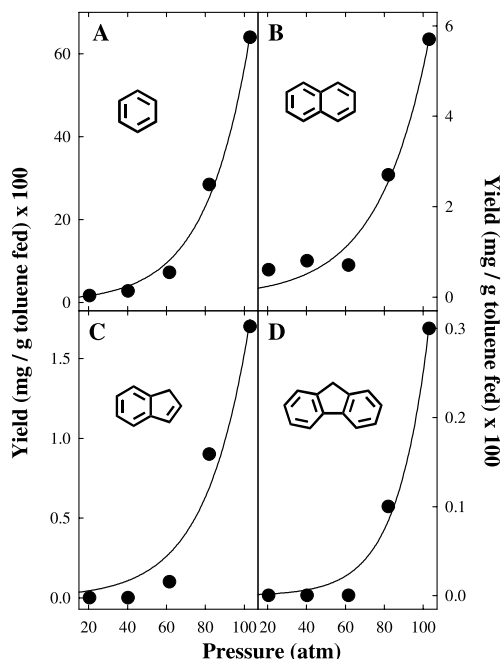


Fig. 2. Yields, versus pressure, from toluene pyrolysis at 535 °C and 140 s: (A) benzene; (B) naphthalene; (C) indene; and (D) fluorene. Circles, experimental data. Curves, fits of the data to Eq. (5).

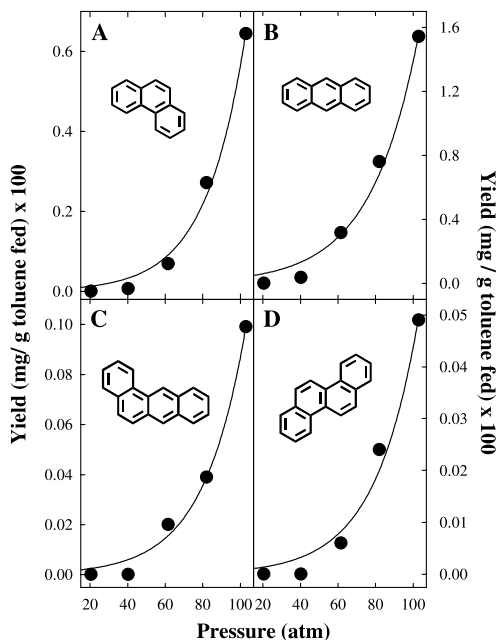


Fig. 3. Yields, versus pressure, from toluene pyrolysis at 535 °C and 140 s: (A) phenanthrene; (B) anthracene; (C) benz[*a*]anthracene; and (D) chrysene. Circles, experimental data. Curves, fits of the data to Eq. (5).

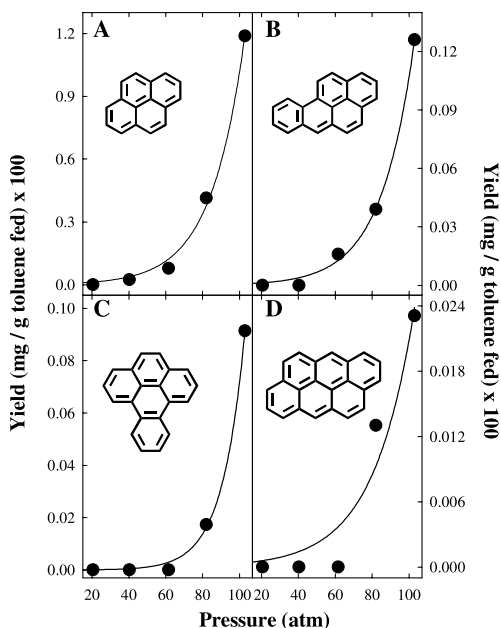


Fig. 4. Yields, versus pressure, from toluene pyrolysis at 535 °C and 140 s: (A) pyrene; (B) benzo[*a*]pyrene; (C) benzo[*e*]pyrene; and (D) anthanthrene. Circles, experimental data. Curves, fits of the data to Eq. (5).

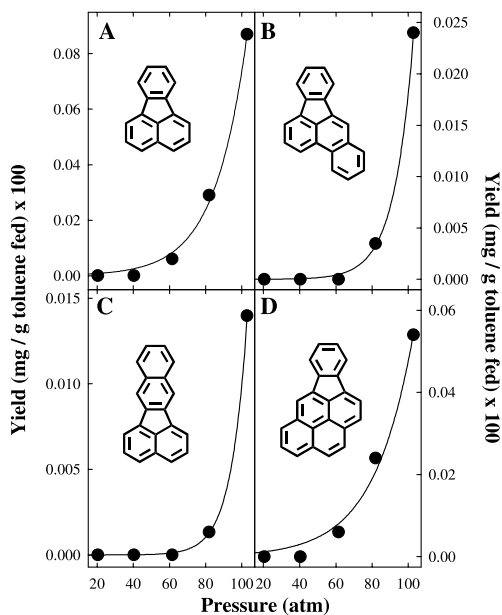


Fig. 5. Yields, versus pressure, from toluene pyrolysis at 535 °C and 140 s: (A) fluoranthene; (B) benzo[*b*]fluoranthene; (C) benzo[*k*]fluoranthene; and (D) indeno[1,2,3-*cd*]pyrene. Circles, experimental data. Curves, fits of the data to Eq. (5).

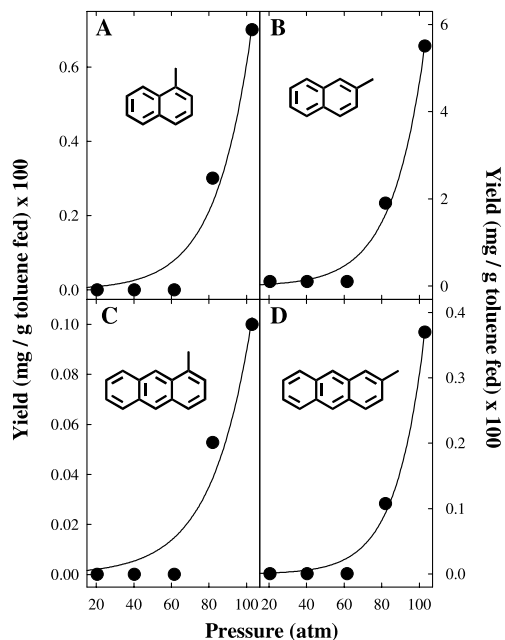


Fig. 7. Yields, versus pressure, from toluene pyrolysis at 535 °C and 140 s: (A) 1-methylnaphthalene; (B) 2-methylnaphthalene; (C) 1-methylanthracene; and (D) 2-methylanthracene. Circles, experimental data. Curves, fits of the data to Eq. (5).

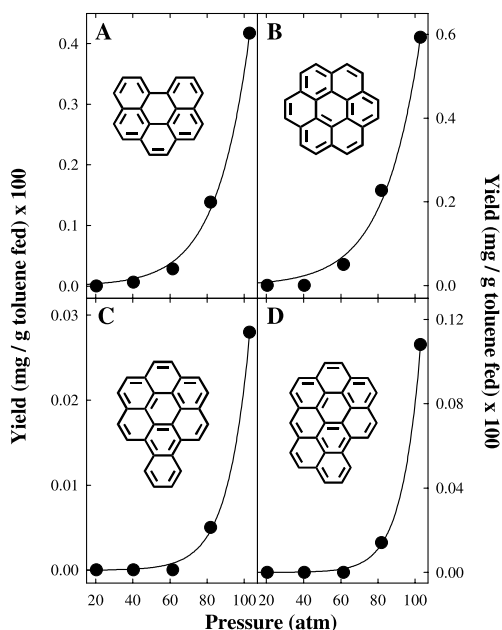


Fig. 6. Yields, versus pressure, from toluene pyrolysis at 535 °C and 140 s: (A) benzo[*ghi*]perylene; (B) coronene; (C) benzo[*a*]coronene; and (D) naphtho[8,1,2-*abc*]coronene. Circles, experimental data. Curves, fits of the data to Eq. (5).

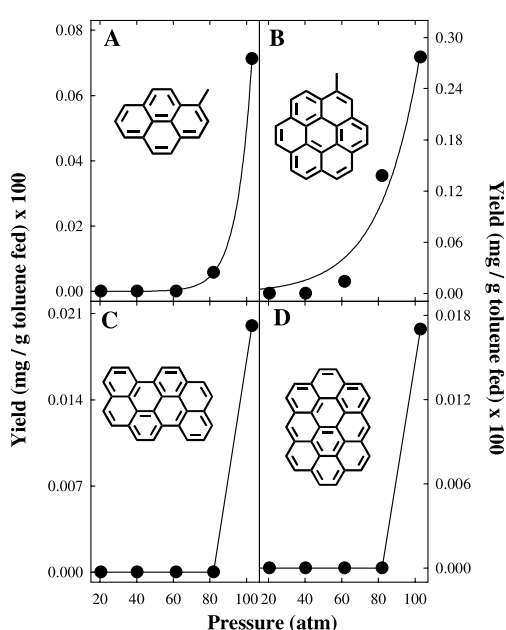


Fig. 8. Yields, versus pressure, from toluene pyrolysis at 535 °C and 140 s: (A) 1-methylpyrene; (B) 1-methylcoronene; (C) benzo[*pqr*]naphtho[8,1,2-*bcd*]perylene; and (D) ovalene. Circles, experimental data. Curves for (A) and (B), fits of the data to Eq. (5).

merely connections between the experimentally measured data points, since the two large PAH represented in C and D are measurable only at the highest pressure, 100 atm.

The first thing to notice in Figs. 2–8 is that all of the PAH product yields are low, corresponding to the low level of toluene conversion in our experiments [38]. Even this low level of PAH production is important, however, with regard to the formation of carbonaceous solids. Experiments run at just 50 °C higher than the conditions of Figs. 2–8 result in repeated plugging of our reactor, due to the formation of solid deposits. Under the high-pressure conditions of the toluene pyrolysis environment, therefore, it appears that even small levels of large PAH can serve as kernels for growth leading to carbonaceous solids.

As Figs. 2–8 demonstrate, the experimentally measured yields of all the PAH increase continuously with pressure, rising particularly dramatically at pressures above the toluene critical pressure of 41 atm. These pressure-dependent product yield data, taken at constant temperature and residence time, permit us to determine the pressure dependency of the global kinetic rate constants for formation of PAH during supercritical toluene pyrolysis. For our global kinetic analysis, we assume that the rate of production of each product B is first order in the concentration of toluene A, so

$$d[B]/dt = k[A], \quad (1)$$

where  $k$  is the global kinetic rate constant (in  $s^{-1}$ ) for the formation of B. For the range of conditions examined in our supercritical toluene pyrolysis experiments, the level of toluene conversion is very small, less than 1%, so the concentration of A is effectively constant with time, at its initial value of  $[A]_0$ . Therefore, integration of Eq. (1) over time gives:

$$[B] = k[A]_0 t \quad (2)$$

or

$$[B]/[A]_0 = kt, \quad (3)$$

where  $[B]/[A]_0$  is just the yield of B, as plotted in Figs. 2–8.

For constant temperature (and pressures <1500 atm), the pressure dependency of the rate constant  $k$  is given [10,43] as:

$$k = A \exp[(-\Delta V^\ddagger/RT)p], \quad (4)$$

where  $A$  is the preexponential factor (in  $s^{-1}$ ) and  $\Delta V^\ddagger$  is the activation volume (in L/mol), defined as the difference between the partial molar volumes of the transition state and the reactants [10]. Substitution of Eq. (4) into Eq. (3) gives:

$$[B]/[A]_0 = At \{ \exp[(-\Delta V^\ddagger/RT)p] \}. \quad (5)$$

Therefore, a set of product yield data at constant temperature and residence time but varying pressures lends itself to determining  $\Delta V^\ddagger$  and  $A$ , if the data conform to the assumed first-order global kinetics.

Using the data from our supercritical toluene pyrolysis at 535 °C and 140 s, we fit the experimentally measured yield/pressure data for each product to Eq. (5), determining the values of  $\Delta V^\ddagger$  and  $A$  that best fit the data for each product species. A yield/pressure curve is then generated from the derived values of  $\Delta V^\ddagger$  and  $A$ , to examine how well the experimental data conform to the assumed first-order behavior.

The curves in Figs. 2–7 and 8A and B, and the values in Table 1 show the results of this exercise for the yield data of benzene and 25 of the PAH produced from the supercritical pyrolysis of toluene at 535 °C and 140 s. As mentioned before, each of the filled circles in Figs. 2–8 is an experimentally measured product yield. Each curve in these figures (except Fig. 8C and D) is the one generated from the values of  $\Delta V^\ddagger$  and  $A$  that best fit the data in Eq. (5). The close matching of the data points and curves for almost all of the PAH in Figs. 2–8 shows that the data conform very well to the assumed first-order global kinetics model. Except for anthanthrene (whose yield is difficult to determine with a high degree of accuracy, due to the coincidence of its elution with a change in HPLC mobile phase composition [37])—the high values of the correlation coefficient  $R^2$  in Table 1 show that all 26 of the products in Table 1, from 1-ring to 9-ring aromatics, conform well to this type of first-order global kinetics treatment.

Table 1 also reports the values of  $\ln A$  and  $\Delta V^\ddagger$  that best fit the experimental data for each product. For most of the compounds in Table 1,  $\ln A$  ( $s^{-1}$ ) falls between  $-20$  and  $-30$ , and  $\Delta V^\ddagger$  falls between  $-2.5$  and  $-4$  L/mol. The negative values of  $\Delta V^\ddagger$  of course indicate that higher pressures favor the formation of PAH products, as the experiments demonstrate. The magnitudes of the  $\Delta V^\ddagger$  values in Table 1 are typical for reactions in supercritical fluids (two orders of magnitude higher than for liquid-phase reactions) [10,12].

The activation volumes in Table 1 are good indicators of how highly pressure-sensitive PAH formation is in the supercritical toluene pyrolysis environment. For an activation volume of  $-2.5$  L/mol at 535 °C, it takes an 18.4-atm rise in pressure to double the formation rate of the product PAH; for an activation volume of  $-4$  L/mol, the formation rate doubles with a pressure increase of only 11.5 atm. Some of the larger PAH in Table 1, such as the 8-ring benzo[*a*]coronene and the 9-ring naphtho[8,1,2-*abc*]coronene, exhibit negative activation volumes of an even greater magnitude, underlining the extreme sensitivity to pressure of the formation rates of these



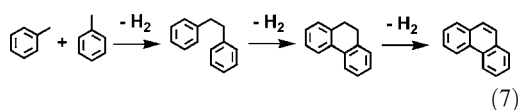
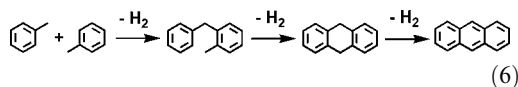
Table 1  
Global kinetic parameters for PAH formation

Aromatic product	$\ln A$ ( $s^{-1}$ )	$\Delta V^\ddagger$ ( $L\text{mol}^{-1}$ )	$R^2$
<i>1- and 2-ring aromatics</i>			
Benzene	−16.8	−2.95	0.993
Indene	−20.4	−2.93	0.963
Naphthalene	−18.6	−2.54	0.980
1-Methylnaphthalene	−22.2	−3.49	0.972
2-Methylnaphthalene	−20.7	−3.83	0.990
<i>3-Ring PAH</i>			
Fluorene	−23.9	−4.03	0.988
Phenanthrene	−21.7	−3.15	0.993
Anthracene	−20.0	−2.61	0.989
1-Methylanthracene	−23.5	−3.10	0.947
2-Methylanthracene	−24.2	−4.36	0.992
<i>4-Ring PAH</i>			
Benz[ <i>a</i> ]anthracene	−23.3	−2.96	0.992
Chrysene	−23.9	−2.88	0.982
Fluoranthene	−24.7	−3.75	0.997
Pyrene	−21.9	−3.64	0.997
1-Methylpyrene	−31.4	−7.95	0.999
<i>5- and 6-ring PAH</i>			
Benzo[ <i>a</i> ]pyrene	−24.2	−3.66	0.998
Benzo[ <i>e</i> ]pyrene	−27.3	−5.46	0.998
Benzo[ <i>b</i> ]fluoranthene	−29.9	−6.25	0.999
Benzo[ <i>k</i> ]fluoranthene	−32.4	−7.49	0.999
Indeno[1,2,3- <i>cd</i> ]pyrene	−24.1	−3.06	0.989
Anthanthrene	−24.8	−2.97	0.936
Benzo[ <i>ghi</i> ]perylene	−23.1	−3.74	0.998
<i>7-, 8-, and 9-ring PAH</i>			
Coronene	−22.2	−3.41	0.994
1-Methylcoronene	−22.4	−3.05	0.969
Benzo[ <i>a</i> ]coronene	−28.8	−5.64	0.999
Naphtho[8,1,2- <i>abc</i> ]coronene	−28.8	−6.56	0.999

large PAH. This result is of particular relevance to the formation of carbonaceous solid deposits, as large PAH are thought to be precursors to these solids [4].

The PAH product yield data of Figs. 2–8 also reveal some results peculiar to the high-pressure toluene pyrolysis environment. For example, unlike results observed for toluene [17] or other fuels [28–31] at atmospheric pressure, Fig. 3 reveals that in the supercritical toluene experiments, yields of anthracene exceed those of its  $C_{14}H_{10}$  isomer phenanthrene. A similar finding is reported [16] for toluene pyrolysis at 10 atm. Both of these  $C_{14}H_{10}$  PAH, anthracene and phenanthrene, can result from the combination of two toluene units, as illustrated in Eqs. (6) and (7) (adopted and extended from Colket and Seery [16]). If anthracene and phenanthrene are formed as Eqs. (6) and (7) suggest, the observed dominance of anthracene over phenanthrene would indicate that at high pressures, union of a benzylic carbon to an aryl site of toluene (Eq. (6)) is preferred over union at two benzylic sites (Eq. (7)). This observation on the relative yields of the  $C_{14}H_{10}$  PAH illustrates the importance of pressure in determining the reaction pathway. The dominance of pyrene

(Fig. 4) over its  $C_{16}H_{10}$  isomer fluoranthene (Fig. 5) and the dominance of benzo[*ghi*]perylene (Fig. 6) over its  $C_{22}H_{12}$  isomer indeno[1,2,3-*cd*]pyrene (Fig. 5) are also results peculiar to this high-pressure environment and contrary to observations in atmospheric-pressure pyrolysis systems [22,28–31]. These differences in relative abundances within isomer families suggest that the mechanisms for PAH formation in the high-pressure environment differ from those in atmospheric-pressure environments. For a discussion of the reaction mechanisms that appear to be responsible for the formation of PAH in the supercritical toluene pyrolysis environment—and the experimental results supporting the proposed mechanisms—the reader is referred to our forthcoming paper [38].



## Acknowledgments

For support of this research, the authors gratefully acknowledge the United States Air Force Office of Scientific Research, Grant Numbers F49620-00-1-0298 and FA9550-04-1-0005. The authors thank Professor Irv Glassman and Dr. John Stewart, of Princeton University, for their valuable contributions to the initiation of this work. The authors also express their appreciation to Dr. Arthur Lafleur and Ms. Elaine Plummer, of the Massachusetts Institute of Technology; Dr. John Fetzer, of Chevron Research; and Professor Maximilian Zander, of Rütgerswerke, for reference standards and UV spectra of PAH.

## References

- [1] S.P. Heneghan, S. Zabarnick, D.R. Ballal, W.E. Harrison III, *J. Energy Resour. Technol.* 118 (1996) 170–179.
- [2] T. Doughty, J.S. Ervin, T.F. Williams, J. Bento, *Ind. Eng. Chem. Res.* 41 (2002) 5856–5866.
- [3] T. Edwards, S. Zabarnick, *Ind. Eng. Chem. Res.* 32 (1993) 3117–3122.
- [4] J.F. Stewart, *Supercritical Pyrolysis of Endothermic Fuels*. Ph.D. thesis, Department of Mechanical and Aerospace Engineering, Princeton University, 1999.
- [5] C.F. Melius, N.E. Bergan, J.E. Shepherd, *Proc. Combust. Inst.* 23 (1990) 217–223.
- [6] F.-G. Klärner, M.K. Diedrich, A.E. Wigger, in: R. van Eldik, C.D. Hubbard (Eds.), *Chemistry Under Extreme or Non-Classical Conditions*, Wiley and Spektrum Akademischer Verlag, New York and Heidelberg, Germany, 1999, p. 103.
- [7] O. Kajimoto, *Chem. Rev.* 99 (1999) 355–389.
- [8] P.E. Savage, *Chem. Rev.* 99 (1999) 603–621.
- [9] J.F. Brennecke, J.E. Châteauneuf, *Chem. Rev.* 99 (1999) 433–452.
- [10] C.A. Eckert, B.E. Knutson, P.G. Debenedetti, *Nature* 383 (1996) 313–318.
- [11] M.E. Paulaitis, G.C. Alexander, *Pure Appl. Chem.* 59 (1987) 61–68.
- [12] K.P. Johnston, C. Haynes, *AIChE J.* 33 (1987) 2017–2026.
- [13] R.H. Helling, J.W. Tester, *Energy Fuels* 1 (1987) 417–423.
- [14] J.F. Stewart, K. Brezinsky, I. Glassman, *Combust. Sci. Technol.* 136 (1998) 373–390.
- [15] M. Bernabei, R. Reda, R. Galiero, G. Bocchinfuso, *J. Chromatogr. A* 985 (2003) 197–203.
- [16] M.B. Colket, D.J. Seery, *Proc. Combust. Inst.* 25 (1994) 883–891.
- [17] G.M. Badger, T.M. Spotswood, *J. Chem. Soc.* (1960) 4420–4427.
- [18] D.C. Astholz, J. Durant, J. Troe, *Proc. Combust. Inst.* 18 (1981) 885–892.
- [19] M. Braun-Unkhoff, P. Frank, Th. Just, *Proc. Combust. Inst.* 22 (1988) 1053–1061.
- [20] H. Richter, J.B. Howard, *Prog. Energy Combust. Sci.* 26 (2000) 565–608.
- [21] J.B. Howard, *Proc. Combust. Inst.* 23 (1990) 1107–1127.
- [22] M.J. Wornat, A.F. Sarofim, A.L. Lafleur, *Proc. Combust. Inst.* 24 (1992) 955–963.
- [23] M.J. Wornat, B.A. Vernaglia, A.L. Lafleur, E.F. Plummer, K. Taghizadeh, P.F. Nelson, C.-Z. Li, A. Necula, L.T. Scott, *Proc. Combust. Inst.* 27 (1998) 1677–1686.
- [24] E.B. Ledesma, M.A. Kalish, M.J. Wornat, P.F. Nelson, J.C. Mackie, *Energy Fuels* 13 (1999) 1167–1172.
- [25] K. Kohse-Höinghaus, B. Atakan, A. Lamprecht, B.G. Alatorre, M. Kamphus, T. Kasper, N.N. Liu, *Phys. Chem. Chem. Phys.* 4 (2002) 2056–2062.
- [26] H. Richter, T.G. Benish, O.A. Mazzyar, W.H. Green, J.B. Howard, *Proc. Combust. Inst.* 28 (2000) 2609–2618.
- [27] H. Wang, M. Frenklach, *Combust. Flame* 110 (1997) 173–221.
- [28] N.D. Marsh, D. Zhu, M.J. Wornat, *Proc. Combust. Inst.* 27 (1998) 1897–1905.
- [29] M.J. Wornat, E.B. Ledesma, N.D. Marsh, *Fuel* 80 (2001) 1711–1726.
- [30] N.D. Marsh, E.B. Ledesma, A.K. Sandrowitz, M.J. Wornat, *Energy Fuels* 18 (2004) 209–217.
- [31] B.A. Vernaglia, M.J. Wornat, C.-Z. Li, P.F. Nelson, *Proc. Combust. Inst.* 26 (1996) 3287–3294.
- [32] A.L. Lafleur, J.B. Howard, K. Taghizadeh, E.F. Plummer, L.T. Scott, A. Necula, K.C. Swallow, *J. Phys. Chem.* 100 (1996) 17421–17428.
- [33] A.L. Lafleur, K. Taghizadeh, J.B. Howard, J.F. Anacleto, M.A. Quilliam, *J. Am. Soc. Mass Spectrom.* 7 (1996) 276–286.
- [34] H. Bockhorn, F. Fetting, H.W. Wenz, *Berichte der Bunsen-Gesellschaft—Physical Chemistry Chemical Physics* 87 (1983) 1067–1073.
- [35] M. Frenklach, D.W. Clary, W.C.J. Gardiner, S.E. Stein, *Proc. Combust. Inst.* 20 (1984) 887–901.
- [36] G.D. Davis, *An Experimental Study of Supercritical Methylcyclohexane Pyrolysis*, M.S.E. thesis, Department of Mechanical and Aerospace Engineering, Princeton University, 1994.
- [37] M.J. Wornat, E.B. Ledesma, P.G. Felton, *Polycyclic Aromat. Comp.* (to be submitted).
- [38] E.B. Ledesma, P.G. Felton, M.J. Wornat, *Energy Fuels* (to be submitted).
- [39] A.H. Cutler, M.J. Antal, M. Jones, *Ind. Eng. Chem. Res.* 27 (1988) 691–697.
- [40] J.C.Y. Lee, *Simulations of Two-Dimensional Chemically Reactive Flows: Flow Past a Fuel Particle and Inside a Reactor Tube*, Ph.D. thesis, Department of Mechanical and Aerospace Engineering, Princeton University, 1996.
- [41] M.J. Wornat, A.L. Lafleur, A.F. Sarofim, *Polycyclic Aromat. Comp.* 3 (1993) 149–161.
- [42] E.V. Dose, G. Guiochon, *Anal. Chem.* 61 (1989) 2571–2579.
- [43] C.D. Hubbard, R. van Eldik, in: R. van Eldik, C.D. Hubbard (Eds.), *Chemistry Under Extreme or Non-Classical Conditions*, Wiley and Spektrum Akademischer Verlag, New York, and Heidelberg, Germany, 1999, p. 53.



## Comments

*Burak Atakan, Universität Duisburg-Essen, Germany.*

Rates of chemical reactions usually depend on concentration and pressure. Could it be that the reactions you are seeing are mainly due to increased concentrations? Do you see a possibility to separate those two effects?

*Reply.* We do believe that both pressure and concentration play important roles in the formation of PAH in the supercritical toluene pyrolysis reaction environment. As pointed out by Stewart ([4,14] in paper), the high pressure retards the diffusional escape of fragment species liberated by pyrolytic bond cleavage and facilitates bond formation by forcing constituent species to have contact with one another. It is because the constituent species are aromatic hydrocarbons in high concentration that this forced contact results in PAH formation in our system. Currently our experiments are run with no diluent fluid, so supercritical toluene is both the reaction medium and the primary reactant, and the effects of pressure and concentration are inseparable. The effects of pressure could be isolated from those of concentration, however, if we were able to perform the toluene experiments in an inert fluid whose critical properties closely simulated those of toluene. Such experiments would permit us to achieve the same pressure effects as in the current experiments, but without the high reactant concentrations.

•

*Houston Miller, George Washington University, USA.*

Your proposed intermediates should be single aromatic rings joined by aliphatic bridges. I understand that these bonds are quite weak due to the stability of benzylic radicals. Have you followed the energetics along the paths that you propose for the formation of fused ring structures?

*Reply.* We have not yet performed calculations of the potential energy surfaces, but we are considering such calculations in our plans for future work.

•

*Phillip R. Westmoreland, University of Massachusetts Amherst, USA.* The largest PAH that you showed which

contained a five-membered ring was an indenopyrene, yet you showed much larger PAH as well. Are C<sub>5</sub>-ring PAH absent in the larger PAH, or is it an inability to identify such species (e.g., for lack of pure-species standards)?

*Reply.* Combustion and pyrolysis systems generally produce three different classes of PAH with five-membered rings: cyclopenta-fused PAH, in which the five-membered ring is on the periphery of the molecule; fluoranthene benzologues, in which the five-membered ring is internal; and indene benzologues, in which the five-membered ring contains a methylene carbon. We consider each of these classes separately. For the cyclopenta-fused PAH, we have an extensive collection of reference standards for species up to nine aromatic rings, but no cyclopenta-fused PAH of any ring number appear in supercritical toluene pyrolysis. This result is not surprising, since cyclopenta-fused PAH are thought [23 in paper] to arise from acetylene addition and the moderate temperature (535°C) of our toluene experiments is too low for acetylene to be formed. We have identified two indene benzologues, but we have only a very limited number of reference standards in this class of PAH. Therefore our failure to identify larger-ring-number species among the indene benzologues does not necessarily mean these products are not formed. Third, with regard to the fluoranthene benzologues, we have identified four products—the largest being the C<sub>22</sub>H<sub>12</sub> indeno[1,2,3-*cd*]pyrene referenced in the question. We have reference standards of a number of C<sub>24</sub>H<sub>14</sub> and C<sub>28</sub>H<sub>16</sub> fluoranthene benzologues, and we have observed such PAH, with the same analytical methods, in the pyrolysis products of coal ([29] in paper) and anthracene ([22] in paper). However, we do not see these particular fluoranthene benzologues in our supercritical toluene pyrolysis products. This result—along with the unusual observation that fluoranthene itself appears in far lower yield than its isomer pyrene—tempts us to conclude that fluoranthene benzologues as a class are not favored as products in the supercritical toluene pyrolysis. Our assessment must be tempered, however, with the realization that there are over a hundred C<sub>24</sub>H<sub>14</sub> and C<sub>28</sub>H<sub>16</sub> fluoranthene benzologues for which reference standards are not available.